CrystEngComm

Accepted Manuscript

ROYAL SOCIETY OF CHEMISTRY

www.rsc.org/crystengcomm

Journal Name

RSCPublishing

COMMUNICATION

Unravelling transient phases during thermal oxidation of copper for dense CuO nanowire growth†

Cite this: DOI: 10.1039/x0xx00000x
Received
Accepted
DOI: 10.1039/x0xx00000x
www.rsc.org/

Fei Wu,[a] Yoon Myung,[a] Parag Banerjee*[a]

Direct evidence of cupric ion outdiffusion through grain boundaries during thermal oxidation of high purity Cu is obtained using Raman spectroscopy. This diffusion feeds the growth of CuO nanowires on the surface while forming $Cu_{1+x}O$ phase in the grain boundaries of underlying Cu_2O film. On complete Cu consumption, counter indiffusion of O^{2-} ions converts the entire structure to a CuO film, while viable CuO nanowires still remain on the surface.

Dense, single crystalline CuO nanowires (NWs) have been shown to spontaneously grow during thermal oxidation of pure Cu.[1,2-5] The accepted mechanism for such growth involves the short circuit grain boundary diffusion of cupric ion (Cu^{++}) from the underlying metallic Cu to the top surface. The outdiffusion occurs through a thick underlayer of columnar Cu_2O grains and a thin overlayer of CuO uniaxial grains (referred to as the CuO NW-CuO-Cu_2O-Cu stack).[4, 6-9] Indirect evidence of such mechanism exists, where cold-worked Cu foils with small grain sizes and hence larger volume fraction of grain boundaries have shown to yield higher density and longer CuO NWs.[10-12] Similarly, electric field enhanced growth of CuO NWs leads to higher rates of growth and longer NW lengths.[13] These results point to the important role of grain boundary enabled fast Cu^{++} outdiffusion in spontaneous CuO NW formation during the thermal oxidation of Cu.

In this paper, we show direct evidence of outdiffusion of Cu^{++} from the Cu foil to CuO NWs through grain boundaries by performing Raman spectroscopy on cross-sections of partially and fully oxidized 26 µm rolled Cu foils. When a concentration (and hence, chemical potential) gradient is established between the CuO NW-CuO-Cu_2O-Cu structure, rapid diffusion of Cu^{++} is established via grain boundaries. This flux manifests itself as a $Cu_{1+x}O$ Raman signature in an otherwise pure Cu_2O columnar film. When the metallic Cu is completely consumed, O^{2-} indiffusion converts the entire sub-layer structure to CuO.

Experimentally, 127 µm thick Cu foils (Alfa Aesar®) with a purity of 99.9 % were rolled to 26 µm. The rolled Cu was cut into 1 cm×0.5 cm pieces. Surface native oxide was removed with 1 M HCl. The cleaned foils were oxidized at 500 °C, 600 °C and 700 °C for 1, 5 and 10 hours (details provided in ESI†, Fig. S1) in ambient. Samples were cooled in the furnace to room temperature. SEM images were taken using a JEOL-7001LVF. Statistical data on NW density, length and oxide layer thickness below NWs was obtained from SEM images using Image-J software. X-ray diffraction (XRD) was performed on a Rigaku Geigerflex D-MAX/A diffractometer. Raman spectra of the samples were obtained using a Renishaw® in Via Raman Microscope with a spot size < 1 µm^2. The objective of the microscope was 50× with N.A. of 0.75. The wavelength of the laser was 514 nm.

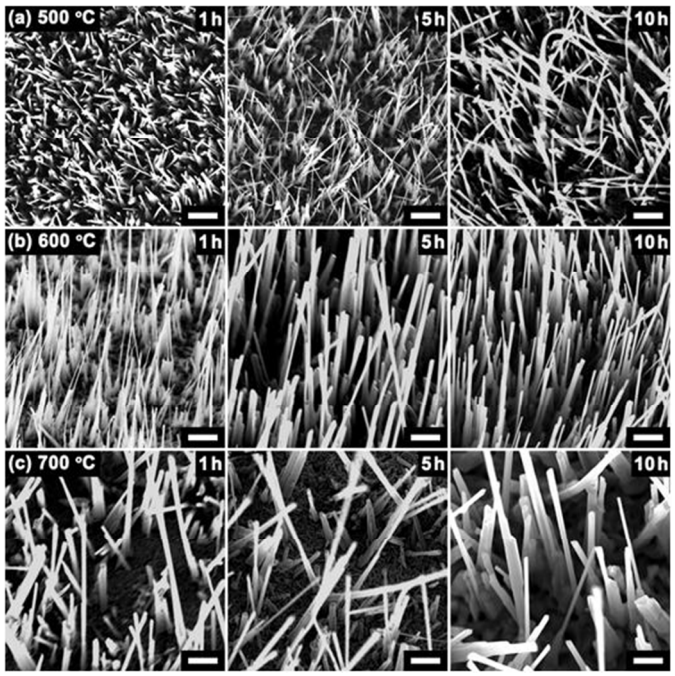

Fig. 1 The SEM images of CuO NWs by oxidizing 26 µm Cu foil in air at 500 °C, 600 °C and 700 °C for 1, 5 and 10 hours, respectively. Scale bars are 1 µm.

SEM images of samples oxidized at 500, 600 and 700 °C for 1, 5 and 10 hours are shown in Fig. 1. Corresponding SEM cross-sections are shown in ESI†, Fig. S2. Statistical averages of NW length, density

*[a]*Department of Mechanical Engineering and Materials Science, Washington University in St. Louis, One Brookings Drive, St. Louis, MO 63130, USA. **Email:** parag.banerjee@wustl.edu.

†Electronic Supplementary Information (ESI) available: Experimental schematic, table of CuO NW parameters, additional SEM and Raman. See DOI: 10.1039/c000000x/

and combined (Cu_2O + CuO) oxide layer thickness below NWs are shown in ESI†, Table S1.

Briefly, we note that viable CuO NWs are formed under all conditions of oxidation. In particular, at 500 ºC, the NW length decreases from 16.3 µm to 8.4 µm as oxidation time is increased from 1 hour to 10 hours. However, NW density remains nearly 1×10^8 cm^{-2} for all oxidation times. At 600 ºC, both the CuO NW density and length increase with oxidation time. The CuO NW density maximizes at 1.7×10^8 cm^{-2} whereas, NW lengths up to 30.9 µm are recorded for 600 ºC, 10 hours. When the oxidation temperature increased to 700 ºC, an increase of oxidation time results in only a modest increase of NW lengths – from 10.1 µm at 1 hour to 13.9 µm at 10 hours. However, NW density reaches a maximum of 1.3×10^8 cm^{-2} at 5 hours and then decreases to 0.3×10^{-8} cm^{-2} for 10 hours. Optimized conditions for very high aspect ratio (average length 30.9 µm: average diameter: 220 nm, aspect ratio ~ 140) NWs seem to be centred around 600 ºC 5 hours.

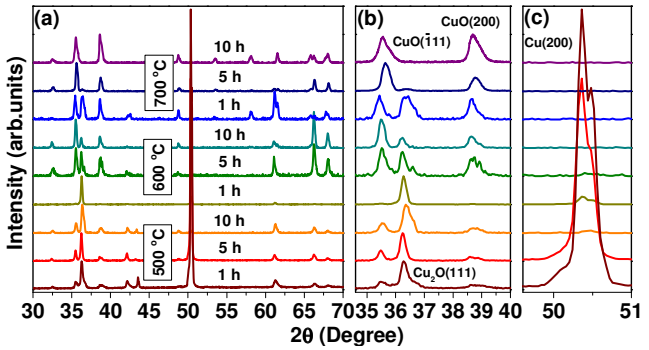

Fig. 2 XRD patterns of (a) Cu foils oxidized at 500-700 ºC for 1-10 hours. Magnified peaks in the range of (b) 2θ = 35-40 degrees and (c) 2θ = 49.5-51.0 degrees to show CuO ($\bar{1}11$),(200), Cu_2O (111) and Cu (200)

Fig. 2(a) shows XRD of the oxidized foils with increasing oxidation temperature and time. The peaks are indexed by the references; CuO (JCPDS No. 80-1916; a=4.692 Å, b=3.428 Å, c=5.137 Å, β=99.546 °), Cu_2O (JCPDS No. 78-2076; a=4.267 Å), and Cu (JCPDS No. 85-1326; a=3.615 Å). First, we focus on the Cu_2O and CuO peak evolution. This is shown in Fig. 2(b). Initially, strong Cu_2O phase is seen at 500 ºC 1 hour. A weaker CuO peak is seen as well originating initially from CuO NWs and the thin CuO overlayer film. Over the course of increasing temperature and time, CuO peaks start to become stronger. In fact, the XRD data for 700 ºC 10 hours shows no Cu_2O and the presence of CuO only. Recall that under these circumstances, robust CuO NWs are still observed on the surface of the oxidized foils (Fig. 1).

Fig. 2(c) shows the enlarged region where metallic Cu peak is expected. Metallic Cu peaks are only observed for 500 ºC 1, 5 and 10 hour samples and for the 600 ºC 1 hour sample. For 600 ºC 5, 10 hours and 700 ºC 1, 5 and 10 hours samples, no Cu signal is recorded. This confirms that all metallic Cu (26 µm thick) is consumed for these samples during oxidation.

The combined SEM and XRD data shows that it is possible to obtain stable and viable CuO NWs on fully converted CuO underlayer films. However, it has been long established that CuO NW formation occurs on CuO NW-CuO-Cu_2O-Cu stack. Our results provide first evidence that under Cu limited growth conditions (such as Cu thin films), a complete conversion of the underlayer to CuO is possible while maintaining the NW structure on top.

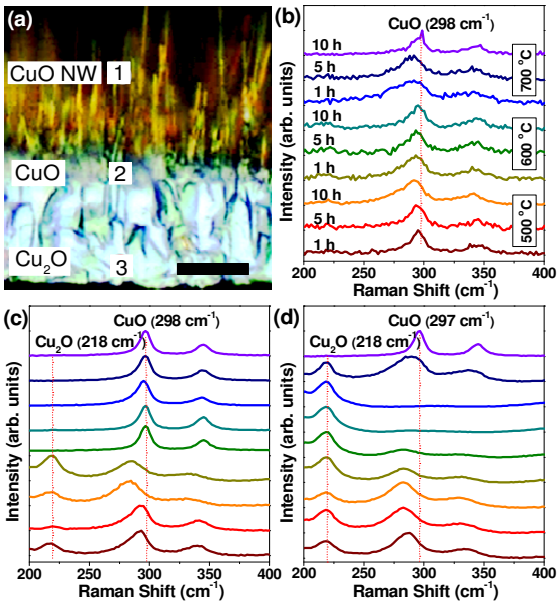

Fig. 3 (a) Representative cross-section of a CuO NW sample under the Raman microscope showing the three spots (1, 2 and 3) from where spectra was acquired in (b), (c) and (d), respectively. Scale bar represents 10 µm.

To study the dynamics of this phase transformation further, micro-Raman spectroscopy was conducted on cross-sections of all the samples. A Raman microscope image of a representative cross-section is shown in Fig. 3(a). Clearly, CuO NWs and two layers of films can be resolved with the microscope. Three ~1 µm diameter spots were chosen to obtain Raman spectra. Spot '1' was chosen within the CuO NWs, spot '2' was chosen at the root of the CuO NWs, while spot '3' was chosen at the bottom of the oxide film.

Spot '1' spectra are shown in Fig. 3(b). As expected, a single peak at 298 cm^{-1} is observed which belongs to the A_g mode for CuO NWs.[14, 15] At spot '2' (Fig. 3(c)), both Cu_2O ($2E_u$ mode at 218 cm^{-1})[16, 17] and CuO are observed for 500 ºC for 1, 5 and 10 hours and 600 ºC for 1 hour samples. Both the CuO and Cu_2O peaks are broad, but the CuO peak is shifted to lower (284 cm^{-1}) wavenumbers. Stress and non-stoichiometry affect the peak position and full width half maximum of the peaks.[18] Further, XRD confirmed remnant metallic Cu in these samples, previously (Fig. 2(c)). For samples 600 ºC 5 hours and 700 ºC 1, 5 and 10 hours, only CuO peaks are observed. These peaks are narrower and centred at 298 cm^{-1} corresponding to a pure CuO phase. These samples do not have any remnant Cu left. Independent of the XRD data, the Raman results confirm that rapid Cu^{++} outdiffusion cause non-stoichiometry in the top oxide film. Once the metallic Cu is consumed, Cu^{++} outdiffusion stops and the film becomes phase pure CuO due to its proximity to the ambient O_2.

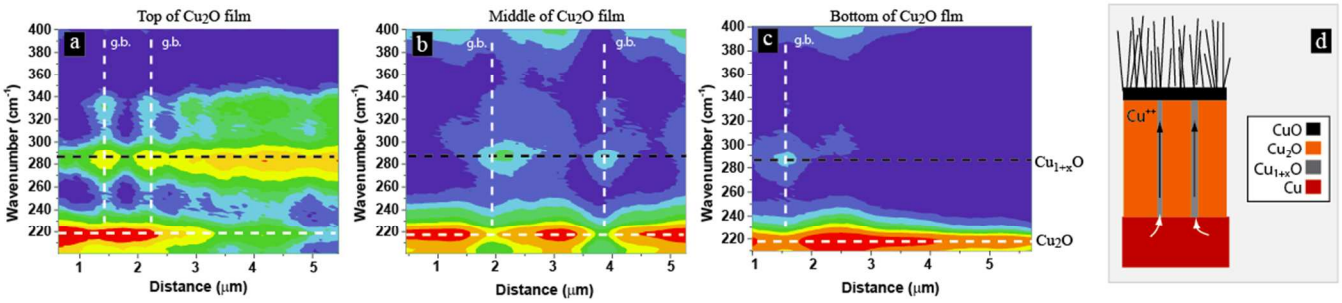

Fig. 4 Raman contour maps through the Cu_2O film for the 500 °C 10 hour sample corresponding to a). Top of the Cu_2O film, b). Middle of Cu_2O film and c). Bottom of Cu_2O film. "g.b." = Grain Boundary. Note: Colour coded intensities are normalized on the log scale to highlight the weaker $Cu_{1+x}O$ signals and d). Schematic of cross section and phases observed during Cu oxidation. The presence of $Cu_{1+x}O$ is seen in the grain boundaries for as long as Cu^{++} ions are supplied from the underlying Cu substrate.

Likewise, at spot '3' (Fig. 3(d)), CuO + Cu_2O phases are seen as well. As in the case of spot '2', the CuO peaks are broader and shift to lower wave numbers (up to 284 cm^{-1}). However, one crucial difference exist which highlight the positional dependence of Cu^{++} out diffusion process in the lower oxide film. The CuO peaks emerge for 500 °C 1, 5 and 10 hours and 600 °C 1 and 5 hour samples, disappear for the 600 °C 10 hours and 700 °C 1 hour samples and then re-emerge for 700 °C 5 and 10 hour samples as sharper peaks at 298 cm^{-1}. The emergence of the early broad CuO red-shifted peak is related to the Cu^{++} ion outdiffusion and the late, sharper CuO peaks are related to the diffusion of O^{2-} front inwards converting Cu_2O to stoichiometric CuO.[16, 18, 19] This result correlates well with the XRD data in Fig. 2b where CuO peaks of increasing intensities occur for 700 °C oxidized samples indicating increasing degree of conversion of the foil to single phase CuO.

To further clarify the location of the broad CuO peaks in the Cu_2O film, we conduct Raman line scans of the underlying Cu_2O film. Fig. 4 (a-c) shows the Raman intensity maps on a 500 °C 10 hour sample (i.e., with Cu remaining) at the top, middle and bottom of the Cu_2O film, respectively (where, X-axis is distance scanned parallel to the film and Y-axis is the Raman shift in wavenumbers). It can be clearly seen that in instances where the laser traverses between two Cu_2O grains (drop in Cu_2O intensity shown as vertical, dotted lines), the CuO signal becomes stronger. Further, the peak position of the CuO is not at 298 cm^{-1} but around 286 cm^{-1} indicating that the CuO is off-stoichiometric ($Cu_{1+x}O$).[20] Thus, off-stoichiometric $Cu_{1+x}O$ observed inside Cu_2O films lies in the grain boundaries of the Cu_2O columnar film and is formed as a result of the rapid and large flux of Cu^{++} diffusing upwards through the grain boundary. A schematic of this situation is shown in Fig. 4(d). Independently, we have verified that when all Cu is consumed, the Cu_2O film reverts to a phase-pure CuO state (see ESI†, Fig. S3).

In summary, we have investigated the thermal oxidation of 26 μm Cu foils to form dense (1.7×10^8 cm^{-2}) and long (up to 30.9 μm and aspect ratio of ~ 140) CuO NWs. This thickness of the foil has allowed us to visualize fast Cu^{++} diffusion through the grain boundaries and study its impact on the stoichiometry of the underlying oxide films. We believe the bilayer oxide interface forms as a result of competitive cation (Cu^{++}) and anion (O^{2-}) counter diffusion. The interface can be controlled and modulated by the relative fluxes of these two species. When Cu feeds the growth of CuO NWs, the CuO and Cu_2O underlayer films are not phase pure as is traditionally reported, but contains a transient (perhaps metastable), off-stoichiometric $Cu_{1+x}O$ phase residing in the grain boundaries – kinetically driven by the fast Cu^{++} outdiffusion. When all Cu is consumed, the films return to their phase pure state. Further oxidation causes continued O^{2-} indiffusion from ambient and the stack is converted from CuO NW-CuO-Cu_2O→CuO NW-CuO. Oxidation under Cu limited growth conditions can thus lead to compositionally homogeneous structures composed of CuO NW – CuO films with wide applicability as photocatalysts, photoelectrodes and as energy harvesting materials.

Acknowledgements

Funding from McDonnell Academy Global Energy and Environment Partnership (MAGEEP) and the International Center for Advanced Renewable Energy & Sustainability (I-CARES) is acknowledged. Microscopy facilities were provided by the Institute of Materials Science and Engineering, Washington University in St. Louis. Thanks to Professor Srikanth Singamaneni (Mechanical Engineering & Materials Science) and Mr. Paul Carpenter (Earth & Planetary Sciences) for providing Raman and XRD facilities.

Notes and References

1. X. C. Jiang, T. Herricks and Y. N. Xia, *Nano Lett*, 2002, **2**, 1333-1338.
2. F. R. N. J. Nabarro, P. J., *Growth of Crystal Whiskers. In Growth and Perfection of Crystal Growth; Doremus, R. H., Roberts, B. W., Turnbull, D., Eds.; Wiley: New York, 1958; pp 13-120.*
3. B. J. Hansen, N. Kouklin, G. H. Lu, I. K. Lin, J. H. Chen and X. Zhang, *J. Phys. Chem. C*, 2010, **114**, 2440-2447.
4. A. M. B. Gonc□alves, L. C. Campos, A. S. Ferlauto and R. G. Lacerda, *J. Appl. Phys.*, 2009, **106**, 034303.
5. A. Kumar, A. K. Srivastava, P. Tiwari and R. V. Nandedkar, *J. Phys.: Condensed Matter*, 2004, **16**, 8531-8543.
6. L. Yuan, Y. Wang, R. Mema and G. Zhou, *Acta Mater.*, 2011, **59**, 2491-2500.
7. B. J. Hansen, H.-l. Chan, J. Lu, G. Lu and J. Chen, *Chem. Phys. Lett.*, 2011, **504**, 41-45.
8. M. L. Zhong, D. C. Zeng, Z. W. Liu, H. Y. Yu, X. C. Zhong and W. Q. Qiu, *Acta Mater.*, 2010, **58**, 5926-5932.
9. Y. Zhu, K. Mimura and M. Isshiki, *Oxidation of Metals*, 2004, **62**, 207-222.
10. R. Mema, L. Yuan, Q. Du, Y. Wang and G. Zhou, *Chem. Phys. Lett.*, 2011, **512**, 87-91.
11. L. Yuan and G. Zhou, *J. Electrochem. Soc.*, 2012, **159**, C205.
12. B. J. Hansen, H. L. Chan, J. A. Lu, G. H. Lu and J. H. Chen, *Chem. Phys. Lett.*, 2011, **504**, 41-45.

13. X. Li, J. Zhang, Y. Yuan, L. Liao and C. Pan, *J. Appl. Phys.*, 2010, **108**.
14. T. Yu, X. Zhao, Z. X. Shen, Y. H. Wu and W. H. Su, *J. Cryst. Growth*, 2004, **268**, 590-595.
15. M. H. Chou, S. B. Liu, C. Y. Huang, S. Y. Wu and C. L. Cheng, *Appl. Surf. Sci.*, 2008, **254**, 7539-7543.
16. B. K. Meyer, A. Polity, D. Reppin, M. Becker, P. Hering, P. J. Klar, T. Sander, C. Reindl, J. Benz, M. Eickhoff, C. Heiliger, M. Heinemann, J. Blasing, A. Krost, S. Shokovets, C. Muller and C. Ronning, *Phys. Status. Solidi. B*, 2012, **249**, 1487-1509.
17. G. J.-D. H. Solache-Carranco, M. Galvan-Arellano, J. Martinez-Juarez, G. Romero-Paredes, R. Pena-Sierra, *2008 5th International Conference on Electrical Engineering, Computing Science and Automatic Control (CCE2008)*, 2008, 4.
18. G. Gouadec and P. Colomban, *Prog. Cryst. Growth Charact. Mater.*, 2007, **53**, 1-56.
19. G. Burns and B. A. Scott, *Phys. Rev. B*, 1973, **7**, 3088-3101.
20. Y. L. Du, M. S. Zhang, Q. Chen and Z. Yin, *Appl. Phys. a-Mater.*, 2003, **76**, 1099-1103.